Available online at www.sciencedirect.com
SCIENCE DIRECT
Journal of Solid State Chemistry 179 (2006) 917–922
JOURNAL OF SOLID STATE CHEMISTRY
www.elsevier.com/locate/jssc

Pressure-induced phase transition and octahedral tilt system change of Ba_2BiSbO_6

Michael W. Lufaso[a], René B. Macquart[a], Yongjae Lee[b], Thomas Vogt[a], Hans-Conrad zur Loye[a,*]

[a]*Department of Chemistry & Biochemistry, University of South Carolina, 631 Sumter St., Columbia, SC 29208, USA*
[b]*Department of Earth System Sciences, Yonsei University, Seoul 120749, South Korea*

Received 13 September 2005; received in revised form 14 November 2005; accepted 11 December 2005
Available online 18 January 2006

Abstract

High-resolution X-ray synchrotron powder diffraction studies under high-pressure conditions are reported for the ordered double perovskite Ba_2BiSbO_6. Near 4 GPa, the oxide undergoes a pressure-induced phase transition. The symmetry of the material changes during the phase transition from space group $R\bar{3}$ to space group $I2/m$, which is consistent with a change in the octahedral tilting distortion from an $a^-a^-a^-$ type to $a^0b^-b^-$ type using the Glazer notation. A fit of the volume–pressure data using the Birch–Murnagaham equation of state yielded a bulk modulus of 144(8) GPa for the rhombohedral phase.

Keywords: High pressure; Phase transition; Double perovskite

1. Introduction

The perovskite, ABO_3, and perovskite related structures are some of the most explored and important structure types in terms of fundamental, technological, and geological importance. The ideal perovskite structure is composed of a corner sharing octahedral (BO_3) network, with the A-cation occupying the cavities surrounded by a cube of eight corner-sharing BO_6 octahedra that generates a 12-fold (AO_{12}) coordination environment. The composition and structural diversity of perovskites are well known, with nearly every element in the periodic table having been incorporated into this structure—the exception being the noble gases and phosphorous. Research on perovskites has been pursued by a large number of researchers, in part, because of the diverse physical properties and remarkable structural chemistry. Although there are a considerable number of simple perovskites, the total quantity of possible compounds is greatly increased when $A(B_{1-x}B'_x)O_3$ compositions containing multiple metal cations are considered. For such systems it is known that when there is a charge and/or size difference between the B-cations, an ordering can occur. The ordering often results in the double perovskite structure with the general stoichiometry $A_2BB'O_6$, where A is typically an alkaline earth cation or lanthanide cation and B and B' are transition metal or lanthanide cations [1]. In both simple and ordered perovskites, the majority are distorted from the ideal, high symmetry cubic form by an octahedral tilting distortion [2,3]. As these slight distortions are often the origin of important physical properties, including dielectric, electric, magnetic, piezoelectric, and magnetoresistive properties the octahedral tilting in cation ordered perovskites has been previously examined in detail using techniques that include group-theoretical analysis [3–7].

Interestingly, changes in temperature or pressure may induce structural and/or property changes. For example, $LaCoO_3$ undergoes an unusual pressure-induced continuous depopulation of the intermediate ($t_{2g}^5e_g^1$) spin state to a nonmagnetic (t_{2g}^6) spin state [8], while $CaMn_{1-x}Ru_xO_3$ ($x = 0-0.4$) perovskites were investigated at pressures up to 12 kbar where it was found that the applied pressure suppresses ferromagnetism and increases resistivity [9].

*Corresponding author. Fax: +1 803 777 8508.
E-mail address: zurloye@mail.chem.sc.edu (H.-C. zur Loye).

0022-4596/$ - see front matter © 2005 Elsevier Inc. All rights reserved.
doi:10.1016/j.jssc.2005.12.024

Near a pressure of 7.5 GPa an electronic structural transition was reported for Sr_2FeNbO_6 [10], while the series $Sr_2TbRu_{1-x}Ir_xO_6$ was studied by temperature and pressure dependent diffraction techniques, where it was found that $Sr_2TbRu_{0.3}Ir_{0.7}O_6$ exhibited a valence state transition at low pressures [11].

Pressure has also been shown to induce structural changes. In general, pressure has an influence on the octahedral tilt angles and the associated *B*–O–*B* bond angles. For example, the magnitude of the octahedral tilting increases with pressure in $CaSnO_3$ [12]. In contrast, the $GdFeO_3$ and $GdAlO_3$ perovskites become less distorted under high-pressure conditions [13]. The high-pressure behavior of the "$GdFeO_3$" type perovskites was examined in terms of the relative compressibility of the AO_{12} site compared to the BO_6 site [13,14]. In general, the $A^{2+}B^{4+}O_3$ type perovskites become more distorted with pressure while in some cases $A^{3+}B^{3+}O_3$ type perovskites may become less distorted with pressure. The $LnAlO_3$ compounds are particularly interesting in this regard. The $LaAlO_3$ perovskite becomes less distorted as it undergoes a pressure-induced phase transition and change in the octahedral tilting type described with Glazer notation [15], from rhombohedral ($a^-a^-a^-$) to cubic ($a^0a^0a^0$) [16], while, in contrast, $PrAlO_3$ undergoes a pressure-induced phase transition above 8 GPa from rhombohedral ($a^-a^-a^-$) to a more distorted orthorhombic ($a^0b^-b^-$) form. At a pressure of 26 GPa, the orthorhombic (space group *Pbnm*) form of $SmNiO_3$ was reported to transform into space group $R\bar{3}$ [17]. Another type of transition is observed for $Ba_2PrRu_{0.8}Ir_{0.2}O_6$, which was reported to undergo a transition from an ambient pressure monoclinic ($P2_1/n$) ($a^-a^-b^+$) to a high-pressure tetragonal ($P4/mnc$) ($a^0a^0c^+$) structure [18]. A pressure-induced phase transition from untilted cubic (space group $Fm\bar{3}m$) to tilted tetragonal (space group $I4/m$) was reported for Ba_2YTaO_6 [19]. A pressure and temperature-dependent structural study of Ba_2BiTaO_6 found that a first-order rhombohedral ($R\bar{3}$) to monoclinic ($I2/m$) structure transition could be induced by either lowering the temperature or through the application of pressure [20]. To see how the related composition, Ba_2BiSbO_6, containing a main group element, antimony, rather than a transition metal, tantalum, would behave under high pressure, we synthesized this double perovskite; and in this paper we describe the preparation and variable pressure synchrotron X-ray powder diffraction study of the ordered double perovskite Ba_2BiSbO_6.

2. Experimental

Ba_2BiSbO_6 powder was prepared by conventional solid state techniques using appropriate stoichiometric mixtures of $BaCO_3$, Bi_2O_3, and Sb_2O_3 and heating for several days with intermediate regrinding at 850 °C until the diffraction peaks associated with cation ordering no longer changed. The phase purity was established by powder X-ray diffraction using a Rigaku D/max 2200 diffractometer. In situ high-pressure synchrotron X-ray powder diffraction experiments were performed using a diamond anvil cell (DAC) at the X7A beam-line at the National Synchrotron Light Source (NSLS) at Brookhaven National Laboratory (BNL). The primary white beam from the bending magnet was monochromatized and focused using an asymmetrically cut bent Si (1 1 1) crystal. A tungsten wire crosshair was positioned at the center of the goniometer circle and subsequently the position of the incident beam was adjusted to the crosshair. A gas-proportional position-sensitive detector (PSD) was stepped in 0.25° intervals over the angular range of 5–40° in 2θ with counting times of 50–100 s per step. The wavelength of the incident beam (0.62245 Å), PSD zero channel and PSD degrees/channel were determined from a CeO_2 standard (SRM 674). The powdered Ba_2BiSbO_6 sample was loaded into the DAC at ambient pressure and room temperature along with a few small ruby chips. The DAC is based on a modified Merrill-Bassett design and employs two diamonds with 0.5 mm diameter culets on tungsten–carbide supports.

The X-rays are admitted by a 0.5 mm diameter circular aperture, and the exit beam leaves via a 0.5×3.0 mm rectangular tapered slit, oriented perpendicular to the horizontal plane of the diffractometer. The sample chamber is composed of a 60 μm diameter hole made using a spark-erosion method in the center of a 250 μm thick stainless-steel gasket, preindented to 100 μm thickness before erosion. The DAC was placed on the second axis of the diffractometer, and the sample position was adjusted

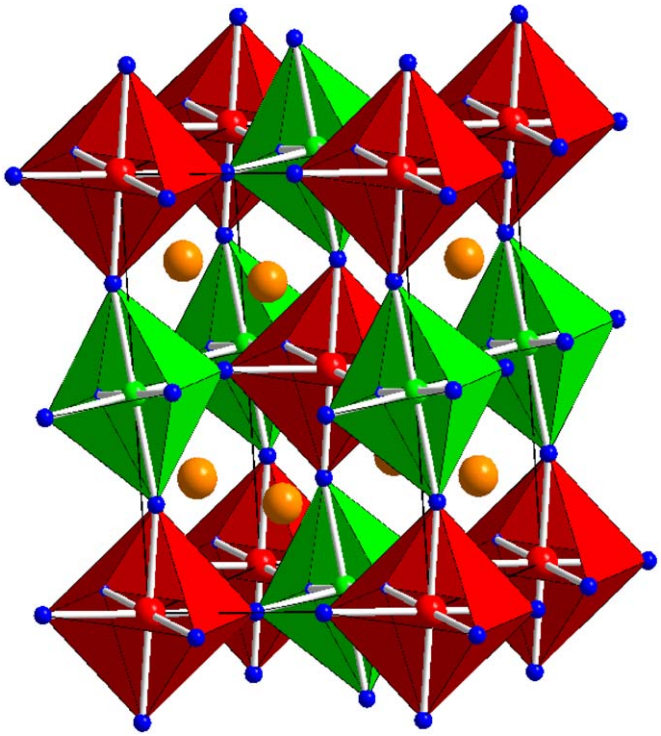

Fig. 1. Crystal structure of Ba_2BiSbO_6 refined in space group $I2/m$ [24]. Orange spheres represent Ba, green spheres Sb, red spheres Bi, and blue spheres O.

using a precentered microscope. The pressure at the sample was measured by detecting the shift in the R1 emission line of the included ruby. No evidence of nonhydrostatic conditions or pressure anisotropy were detected during our experiments, and the R1 peaks from three included ruby chips remained strong and sharp with deviations in the measured pressure of less than 0.1 GPa. A methanol–ethanol–water mixture with component ratio of 16:3:1 was used as a pressure medium. Diffraction data analysis was performed using the EXPGUI interface of GSAS [21,22]. A pseudo-Voight function was used to model the peak shapes. The angular range employed in the refinements was from 6° to 35° 2θ and excluded the regions which contained strong Bragg peaks from the pressure cell gasket.

3. Results and discussion

The structure of Ba_2BiSbO_6 is rhombohedral based on an analysis of the X-ray diffraction data collected at ambient pressure and temperature, and in agreement with the results of Fu [23]. The structure is characterized by a rock-salt like ordering of Bi and Sb, which is combined with an out-of-phase rotation about the pseudocubic [111] axis. The octahedral tilting is the $a^-a^-a^-$ type in the Glazer notation [15]. Although the most commonly observed octahedral tilting distortion type is $a^-a^-b^+$ [2], there are some examples of ordered double perovskites that adopt the $a^-a^-a^-$ type, including $Ba_2Bi(III)Bi(V)O_6$ [24], Ba_2BiSbO_6 [23], Ba_2BiTaO_6 [25], La_2NiMnO_6 [26], and La_2CoMnO_6 [27]. Compounds crystallizing in space group $R\bar{3}$ may undergo a phase transition in which the type of octahedral tilting changes. A first-order phase transition from $R\bar{3} \rightarrow I2/m$ was observed near 425 K in $Ba_2Bi(III)Bi(V)O_6$ [24,28]. The phase transition from rhombohedral $R\bar{3}$ to monoclinic $I2/m$ involves a change in the octahedral tilting type from $a^-a^-a^-$ to $a^0b^-b^-$, respectively. The $R\bar{3}$ ($a^-a^-a^-$) form of $Ba_2Bi(III)Bi(V)O_6$ exists between ~425 and 793 K, above which a phase transition to $Fm\bar{3}m$ ($a^0a^0a^0$) occurs [28–30]. A pressure and temperature-dependent structural study of Ba_2BiTaO_6 found that it undergoes a first-order rhombohedral ($R\bar{3}$) to monoclinic ($I2/m$) structure transition that could be induced by either lowering the temperature or through the application of pressure [20]. A slightly different sequence of phase

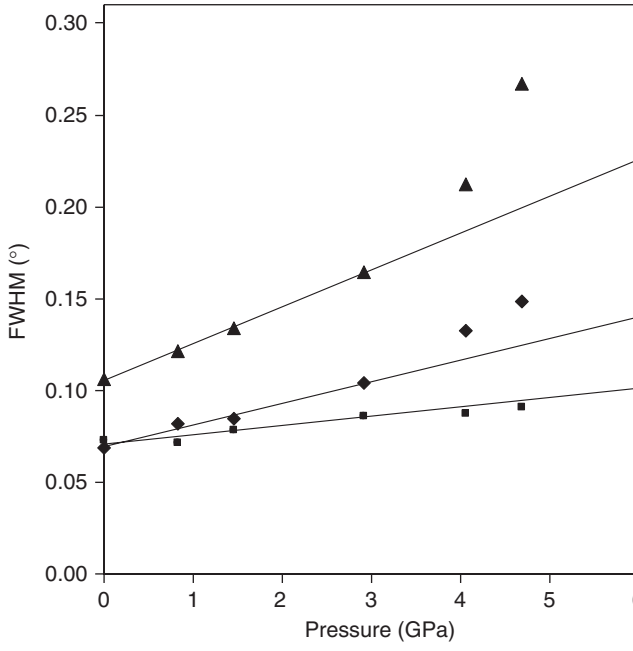

Fig. 2. Pressure dependence of the full-width at half-maximum for diffraction peaks near 8° 2θ (squares), 17° 2θ (diamonds) and 27° 2θ (triangles). Lines are included to guide the eye.

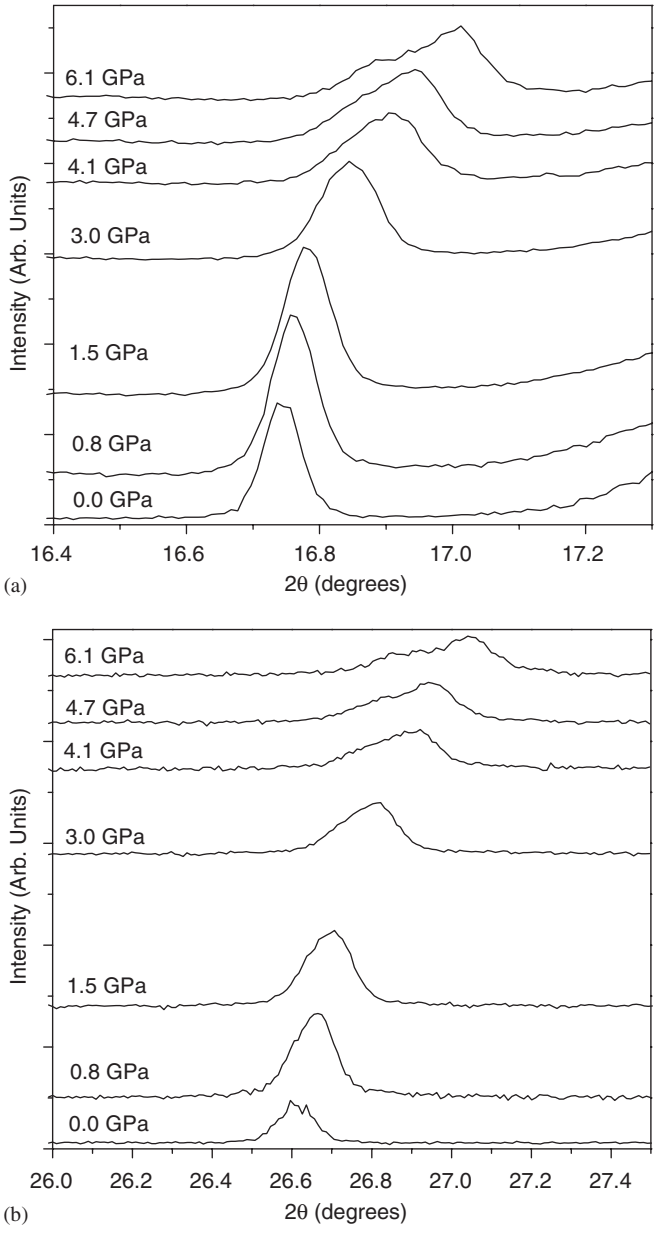

Fig. 3. Pressure dependence of the diffraction peak(s) near 17° 2θ (top) and 27° 2θ (bottom) of Ba_2BiSbO_6.

transitions were reported for La_2NiMnO_6 and La_2CoMnO_6; at 400 K La_2NiMoO_6 was reported to crystallize in space group $R\bar{3}$, whereas at 1.5 K it was reported to crystallize in space group $P2_1/n$ and thus a phase transition from $P2_1/n$ ($a^-a^-b^+$) to $R\bar{3}$ was suggested [26,27]. The $P2_1/n$ to $I2/m$ phase transition can be continous [3] and $I2/m$ may be an intermediate phase in the sequence of transitions for La_2NiMnO_6 and La_2CoMnO_6. The low temperature form of Ba_2BiSbO_6 crystallizes in space group $I2/m$, whereas at room temperature it has $R\bar{3}$ space group symmetry [23,24,31]. The crystal structure of the low temperature form is shown in Fig. 1. It was observed that the application of pressure to Ba_2BiSbO_6 results in a decrease in the lattice parameters. A pressure-induced broadening of the peaks is observed. Fig. 2 shows the full-width at half-maximum (FWHM) for the peaks near 8° 2θ (rhombohedral 0 $\bar{1}$ $\bar{1}$), 17° 2θ (rhombohedral 0 $\bar{2}$ $\bar{2}$) and 27° 2θ rhombohedral 1 3 4 and 1 $\bar{2}$ 3. The FWHM of the low angle peak near 8° 2θ steadily increases with an increase in applied pressure. A relatively linear increase in the FWHM is observed up to 3.0 GPa for the higher angle peaks, at which point the FWHM increases more rapidly. Fig. 3 illustrates the pressure dependence of the peaks near 17° and 27° 2θ. Although the peaks are not well-resolved, it is clear from the analysis of the diffraction data that the peaks are beginning to split into multiple reflections.

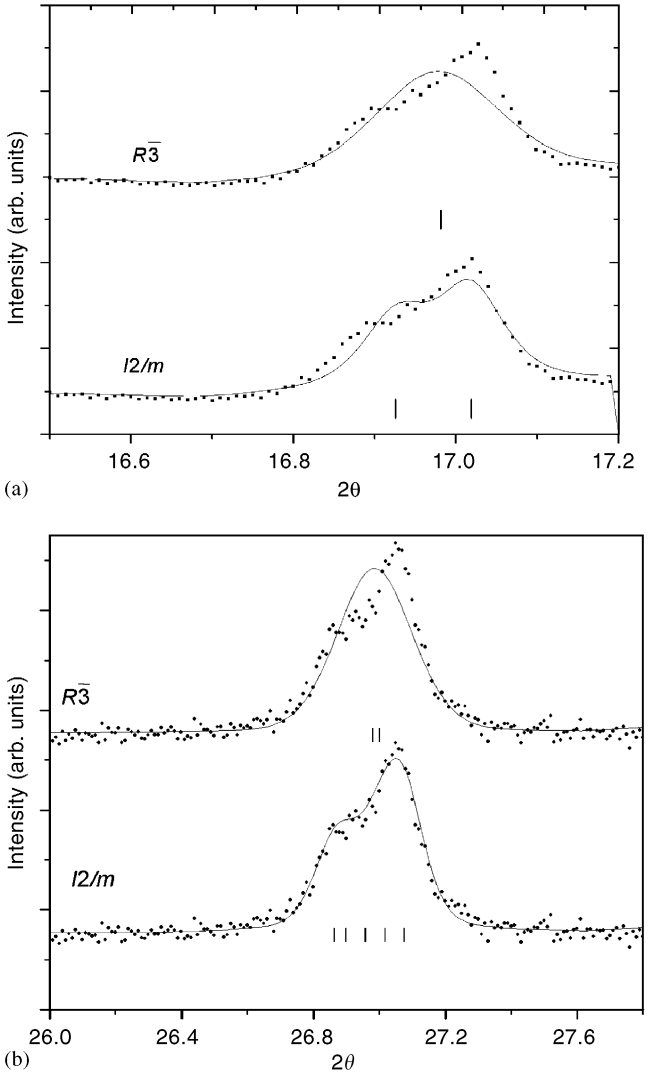

Fig. 4. Fitting of the diffraction peaks near 17° 2θ (top) and 27° 2θ (bottom) in space groups $R\bar{3}$ (top) and $I2/m$ (bottom) at an applied pressure of 6.1 GPa.

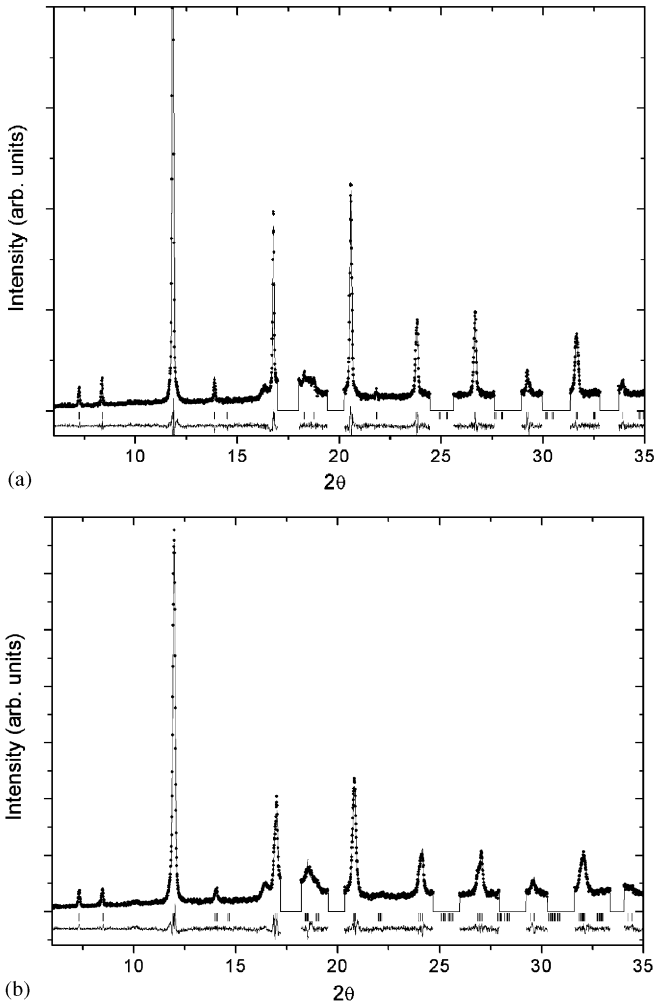

Fig. 5. Observed (circles) and calculated (lines) fitted with the Le Bail method to data collected at a pressure of (top) 0.8 and (bottom) 6.1 GPa. Vertical marks correspond to the Bragg positions for the models with space groups $R\bar{3}$ (top) and $I2/m$ (bottom).

Table 1
Pressure dependence of the lattice parameters and unit cell volume at a pressure up to 3 GPa

Pressure (GPa)	Space group	a (Å)	α (°)	Volume (Å^3)
0.0	$R\bar{3}$	6.05054(14)	59.875(2)	156.182(9)
0.8	$R\bar{3}$	6.0467(4)	59.856(4)	155.817(21)
1.5	$R\bar{3}$	6.0370(2)	59.837(3)	155.006(12)
3.0	$R\bar{3}$	6.0141(2)	59.840(2)	153.254(10)

Table 2
Pressure dependence of the lattice parameters and unit cell volume in the pressure range between 4.1–6.1 GPa

Pressure (GPa)	Space group	a (Å)	b (Å)	c (Å)	β (°)	Volume (Å^3)
4.1	$I2/m$	6.0174(4)	5.9573(5)	8.4559(4)	89.945(7)	303.12(4)
4.7	$I2/m$	6.0059(3)	5.9669(4)	8.4402(5)	89.934(16)	302.47(3)
6.1	$I2/m$	5.9994(5)	5.9640(6)	8.4136(5)	89.713(10)	301.04(4)

Using the Le Bail method, the fitting of the peaks in space groups $R\bar{3}$ and $I2/m$ is shown for the data set collected at an applied pressure of 6.1 GPa. The fit to the data is clearly superior in the $I2/m$ model compared to $R\bar{3}$ and is shown in Fig. 4. There were no indications of any peaks appearing that are associated with in-phase octahedral tilting, which would indicate a tilt system with in-phase octahedral tilting (e.g., space group $P2_1/n$). Space group $I2/m$ was therefore used for the refinements of the cell parameters for data collected at pressures between 4.1 and 6.1 GPa. Representative data sets are shown in Fig. 5 that were collected at a pressure of 0.8 and 6.1 GPa and fitted using the Le Bail method with space groups $R\bar{3}$ and $I2/m$, respectively. The observed phase transition, $R\bar{3} \rightarrow I2/m$, is in agreement with the crystal structures of Ba_2BiSbO_6 reported at ambient and low temperature [23,24], confirming that pressure as well as temperature can induce this structural change. It is worth noting that the $R\bar{3} \rightarrow I2/m$ phase transition was also reported for Ba_2BiTaO_6 [20].

The change in the FWHM shown in Fig. 2 suggests that the phase transition occurs between 3.1 and 4.1 GPa. The pressure dependence of the lattice parameters and unit cell volumes for the $R\bar{3}$ phase up to 3.0 GPa and the $I2/m$ phase between 4.1 and 6.1 GPa are listed in Tables 1 and 2. The pressure dependence of the normalized unit cell volumes are plotted in Fig. 6. The volume decreases with an increase in pressure, a decrease, which is also observed upon lowering the temperature.

The bulk modulus of the rhombohedral phase of Ba_2BiSbO_6 was obtained by fitting a second-order Birch–Murnaghan equation of state to the pressure dependence data up to 3.0 GPa, which is shown by the solid line in Fig. 6. The determined bulk modulus is 144(8) GPa with a V_0 of 156.3(2)Å^3 and is comparable to other ordered double perovskites, for example Ba_2BiTaO_6, $Ba_2PrRu_{0.8}Ir_{0.2}O_6$, and $Sr_2TbRu_{0.3}Ir_{0.7}O_6$, which have bulk moduli of 126(10) GPa [20], 139(10) GPa [18], and 196(10) GPa [11], respectively.

In conclusion, we have performed high-pressure synchrotron powder diffraction experiments on Ba_2BiSbO_6. The structure undergoes a pressure-induced phase transition from space group $R\bar{3}$ to $I2/m$. The phase transition is characterized by a change in the octahedral tilting from an $a^-a^-a^-$ to $a^0b^-b^-$ type. The bulk modulus of 144(8) GPa of the rhombohedral phase is typical for ordered double perovskites.

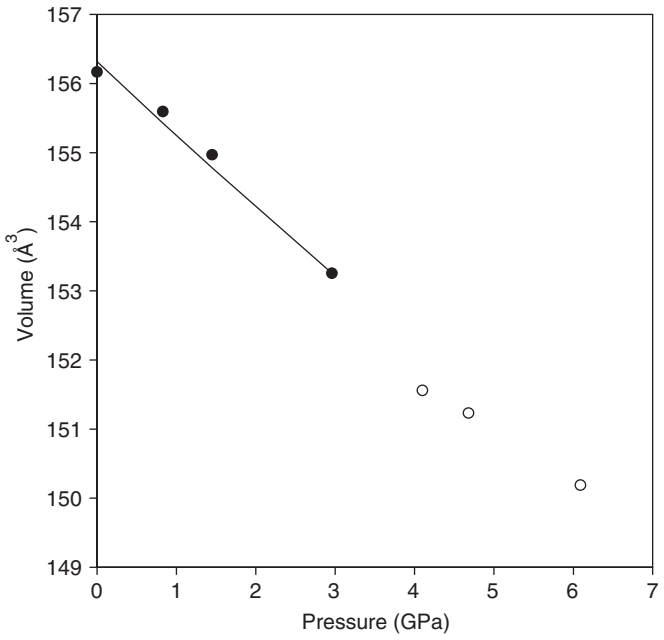

Fig. 6. Pressure dependence of the unit cell volume of Ba_2BiSbO_6. The filled circles are volumes obtained from the fit in $R\bar{3}$ and the open circles are the unit cell volumes obtained from the fit in space group $I2/m$ and normalized by $\frac{1}{2}$ for comparison.

Acknowledgments

Work at Brookhaven is supported by the US Department of Energy, Division of Materials Sciences, under Contract DE-AC02-98CH10886. Financial support from the Department of Energy through Grant DE-FG02-04ER46122 and the National Science Foundation through Grant DMR:0450103 is gratefully acknowledged.

References

[1] R.H. Mitchell, Perovskites: Modern and Ancient, Almaz Press, Ont., Canada, 2002.
[2] M.W. Lufaso, P.M. Woodward, Acta Crystallogr. B 57 (2001) 725–738.
[3] C.J. Howard, B.J. Kennedy, P.M. Woodward, Acta Crystallogr. B 59 (2003) 463–471.
[4] P.M. Woodward, Acta Crystallogr. B 53 (1997) 32–43.
[5] P.M. Woodward, Acta Crystallogr. B 53 (1997) 44–66.
[6] C.J. Howard, H.T. Stokes, Acta Crystallogr. B 54 (1998) 782–789.
[7] C.J. Howard, H.T. Stokes, Acta Crystallogr. B 60 (2004) 674–684.
[8] T. Vogt, J.A. Hriljac, N.C. Hyatt, P.M. Woodward, Phys. Rev. B 67 (2003).

[9] V. Markovich, I. Fita, R. Puzniak, E. Rozenberg, C. Martin, A. Wisniewski, A. Maignan, B. Raveau, Y. Yuzhelevskii, G. Gorodetsky, J. Magn. Magn. Mater. 290 (2005) 898–901.
[10] X. Zhao, R.C. Yu, L.D. Yao, F.Y. Li, Z.X. Liu, Z.X. Bao, X.D. Li, Y.C. Li, M.N. Ma, J. Liu, G.D. Tang, C.Q. Jin, J. Phys.: Condens. Matter 16 (2004) 1299–1305.
[11] Q. Zhou, B.J. Kennedy, K.S. Wallwork, M.M. Elcombe, Y. Lee, T. Vogt, J. Solid State Chem. 178 (2005) 2282–2291.
[12] J. Zhao, N.L. Ross, R.J. Angel, Phys. Chem. Miner. 31 (2004) 299–305.
[13] N.L. Ross, J. Zhao, R.J. Angel, J. Solid State Chem. 177 (2004) 3768–3775.
[14] J. Zhao, N.L. Ross, R.J. Angel, Acta Crystallogr. B-Struct. Sci. 60 (2004) 263–271.
[15] A.M. Glazer, Acta Crystallogr. B 28 (1972) 3384–3392.
[16] P. Bouvier, J. Kreisel, J. Phys.: Condens. Matter 14 (2002) 3981–3991.
[17] M. Amboage, M. Hanfland, J.A. Alonso, M.J. Martinez-Lope, J. Phys.: Condens. Matter 17 (2005) S783–S788.
[18] B.J. Kennedy, L.Q. Li, Y. Lee, T. Vogt, J. Phys.: Condens. Matter 16 (2004) 3295–3301.
[19] M.W. Lufaso, R.B. Macquart, Y. Lee, T. Vogt, H.-C. zur Loye, Chem. Commun. (2006) 168–170.
[20] K.S. Wallwork, B.J. Kennedy, Q.D. Zhou, Y. Lee, T. Vogt, J. Solid State Chem. 178 (2005) 207–211.
[21] A.C. Larson, R.B. von Dreele, General Structure Analysis System (GSAS), Los Alamos National Laboratories, 1990.
[22] B.H. Toby, J. Appl. Crystallogr. 34 (2001) 210–213.
[23] W.T. Fu, Solid State Commun. 116 (2000) 461–464.
[24] G. Thornton, A.J. Jacobson, Acta Crystallogr. B 34 (1978) 351–354.
[25] Q.D. Zhou, B.J. Kennedy, Solid State Sci. 7 (2005) 287–291.
[26] J. Blasco, J. Garcia, M.C. Sanchez, J. Campo, G. Subias, J. Perez-Cacho, Eur. Phys. J. B 30 (2002) 469–479.
[27] C.L. Bull, D. Gleeson, K.S. Knight, J. Phys.:Condens. Matter 15 (2003) 4927–4936.
[28] Q.D. Zhou, B.J. Kennedy, Solid State Commun. 132 (2004) 389–392.
[29] D.E. Cox, A.W. Sleight, Acta Crystallogr. B 35 (1979) 1–10.
[30] S.Y. Pei, J.D. Jorgensen, B. Dabrowski, D.G. Hinks, D.R. Richards, A.W. Mitchell, J.M. Newsam, S.K. Sinha, D. Vaknin, A.J. Jacobson, Phys. Rev. B 41 (1990) 4126–4141.
[31] W.T. Fu, D.J.W. Ijdo, J. Solid State Chem. 128 (1997) 323–325.